

# Plasmon Resonance and Clustering of Silver Nanoclusters Embedded in Glass

J. Ph. Blondeau · F. Catan · C. Andreazza-Vignolle ·  
Nadia Sbai

Received: 12 November 2007 / Accepted: 7 February 2008 / Published online: 5 March 2008  
© Springer Science + Business Media, LLC 2008

**Abstract** Silver nanoclusters growth in AR Schott glass was investigated by transmission electron microscopy (TEM) and optical absorption. The studied samples were Ag–Na ion-exchanged and annealed at ambient air in a furnace. Optical absorption was performed to visualize the size effect on the spectra and compared to the Drude model. TEM was used to evaluate the distribution size of the silver particles so as to confirm the precipitation of the metallic nano-aggregates, to observe their morphological evolution with time, and to correlate it to the absorption curves which makes the interest and the aim of this study. The TEM observations prove that we are in a confinement regime with a particle size below the mean free path of the bulk metal. Growth of the clusters is ascribed first to the diffusion of the silver ions due to annealing and in a second time to an Oswald process.

**Keywords** Silver nano aggregates · Ionic exchange · Plasmon resonance · TEM · Oswald

## Introduction

Synthesis and characterization of nano-sized metallic powders have attracted attention of materials community

due to their promising properties. Nanoscale materials are currently under active research because they possess interesting physical properties differing considerably from that of the bulk phase. Metallic nanoparticles have many potential applications such as heterogeneous catalysts, surfaces of heat exchangers, memory devices, gas sensors, optical waveguide, and optical switches [1–3]. Extensive studies are being conducted on silver nano-sized particles for their commercial application areas such as medical tools, appliances, and health care products [4, 5].

Heterogeneous materials consisting of metallic nanoclusters in amorphous matrices are synthesized by a variety of methods. Low-energy ion beam mixing [6], sol-gel [7], direct metal ion implantation [8], light ion irradiation of ion-exchanged glasses [9–11], annealing of ion-exchanged glasses in hydrogen atmosphere [12], evaporation-condensation [13] are, for example, among these few successful methods to prepare composites of this nature. In this work, ion exchange was used to introduce silver ions in a soda-lime glass. A thermal annealing at room temperature follows this step to promote the silver diffusion and the aggregation. Optical absorption in the UV-visible range have been recorded in function of time. The aim of the present paper was to present the particle size evolution with the annealing time via transmission electron microscopy (TEM) and optical absorption measurements. The absorption curves are here compared to the Drude model and correlated to the growth process and the particles distribution size and shape.

J. P. Blondeau (✉) · F. Catan · N. Sbai  
PRISME, Université d'Orléans,  
21 Rue Loigny La Bataille,  
28000 Chartres, France  
e-mail: jean-philippe.blondeau@univ-orleans.fr

C. Andreazza-Vignolle  
CRMD UMR6619, Université d'Orléans-CNRS,  
1 bis Rue de la Férollerie,  
45071 Orléans, France

## Experimental

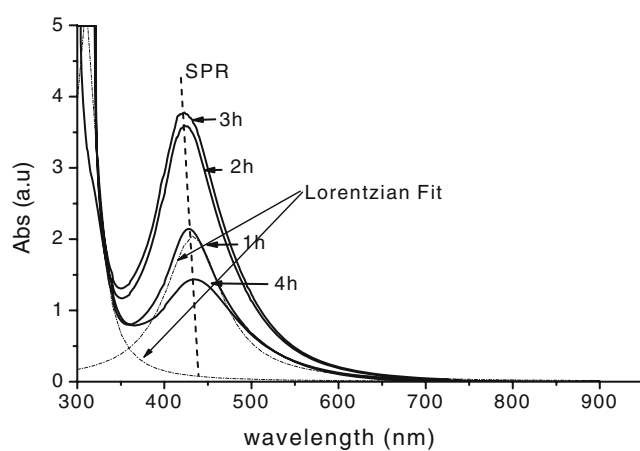
A AR Schott soda-lime glass was chosen as the dielectric medium for embedding the silver nanoparticles. The composition of the glass is 69% SiO<sub>2</sub>, 13% Na<sub>2</sub>O, 4%

$\text{Al}_2\text{O}_3$ , 3%  $\text{K}_2\text{O}$ , 5%  $\text{CaO}$ , 2%  $\text{BaO}$ , 3%  $\text{MgO}$ , and 1%  $\text{B}_2\text{O}_3$  by weight. Silver-exchanged soda glass samples were prepared by immersing the AR glass for 5 h in a molten bath of 6 wt%  $\text{AgNO}_3/\text{NaNO}_3$  mixture at 400 °C. The samples were subsequently annealed at 500 °C for durations between 1 and 4 h. For the annealing, the furnace was preheated at the work temperature. Then, the samples were introduced.

Optical absorption measurements were performed on silver-exchanged glass samples after annealing using a spectrophotometer Jasco UV–Visible V-530, with a resolution of 2 nm, in 300- to 900-nm wavelength range. To determine the size of the silver clusters by direct means, transmission electron microscopy (Philips CM 20 operated at 200 kV) was used. For these measurements, sample was prepared in the following way: sample was polished with a diamond paper for obtaining a few micron thickness containing the silver nanoparticles. A powder was obtained and diluted in ethanol. The solution was agitated by ultrasound for 5 min. A drop was collected on a carbon-coated copper grid for the observations. Furthermore, high-resolution TEM (HRTEM) and electron diffraction was carried out to achieve the particle structure.

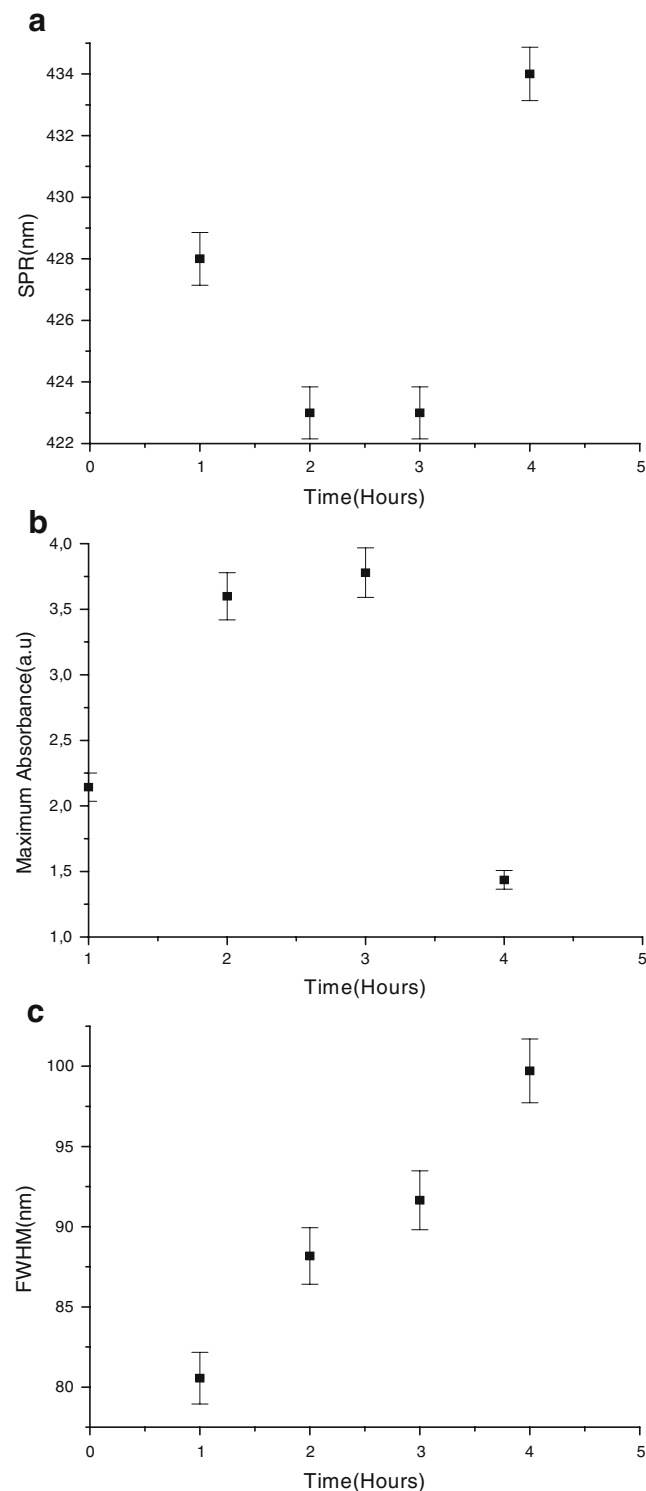
## Results

Figure 1 shows the experimental recorded optical absorption spectra for different annealing times. The optical resonance absorption observed in the spectra is due to the collective oscillations of the conduction electrons with respect to the ionic background in the nanoscale silver particles. The spectra follow the same overall trend of increasing intensity with increasing annealing time, except for 4 h. Peak position



**Fig. 1** Optical absorption spectra of silver nanoparticles embedded in silver-exchanged AR glass matrix after annealing at 500 °C for different times. The dashed line shows the position of the SPR. Dashed dots are used for the fitted data

of the optical response of the matrix-embedded silver nanoparticles is observed to be weak and sensitive to time variation. A very weak blue shift of the surface plasmon resonance (SPR) was observed for samples heated from 1 up



**Fig. 2** SPR (a), maximum absorbance (b), and FWHM (c) evolution with time

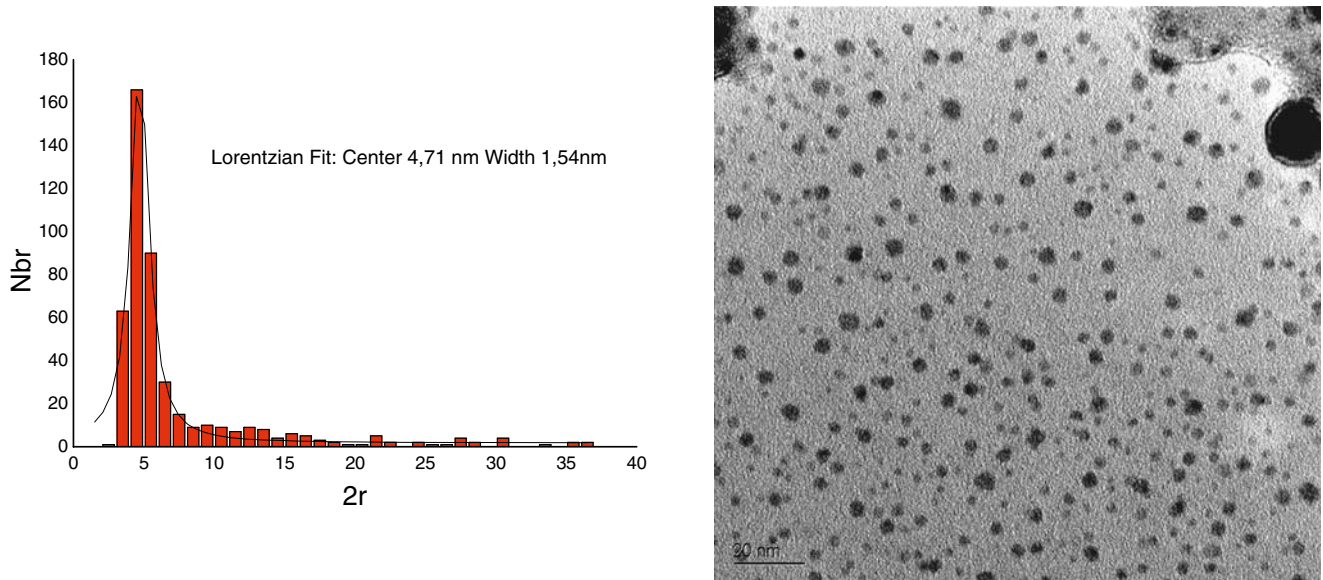


**Fig. 3** Size distribution of the sample annealed for 1 h. A Lorentzian law is used to fit the distribution

to 3 h (Fig. 2a). For the 4-h sample, a red shift of the SPR occurred. For this sample, the intensity which previously increases fell considerably (Fig. 2b) according to the Drude model (see “[Discussion](#)”). For annealing times between 1 and 4 h, the full-width half-maximum (FWHM) obtained with a Lorentzian fit is broadened from 80 to 100 nm (Fig. 2c). This bandwidth allows us to estimate the particle size in the nanometer range from the approximate formula  $R = V_f / \Delta\omega$ , with  $V_f$  the Fermi velocity of electrons in bulk

silver and  $\Delta\omega$  the bandwidth of the fitted absorption curves. The size deduced from this formula is about 1.7 nm for a 80-nm FWHM and gives an estimation of the size range, but is below the TEM observations.

To understand the optical absorption evolution, TEM analyses of the samples were performed. To fit the size distribution evolution versus annealing time, we used either Gaussian or Lorentzian law according to origin data analysis software.

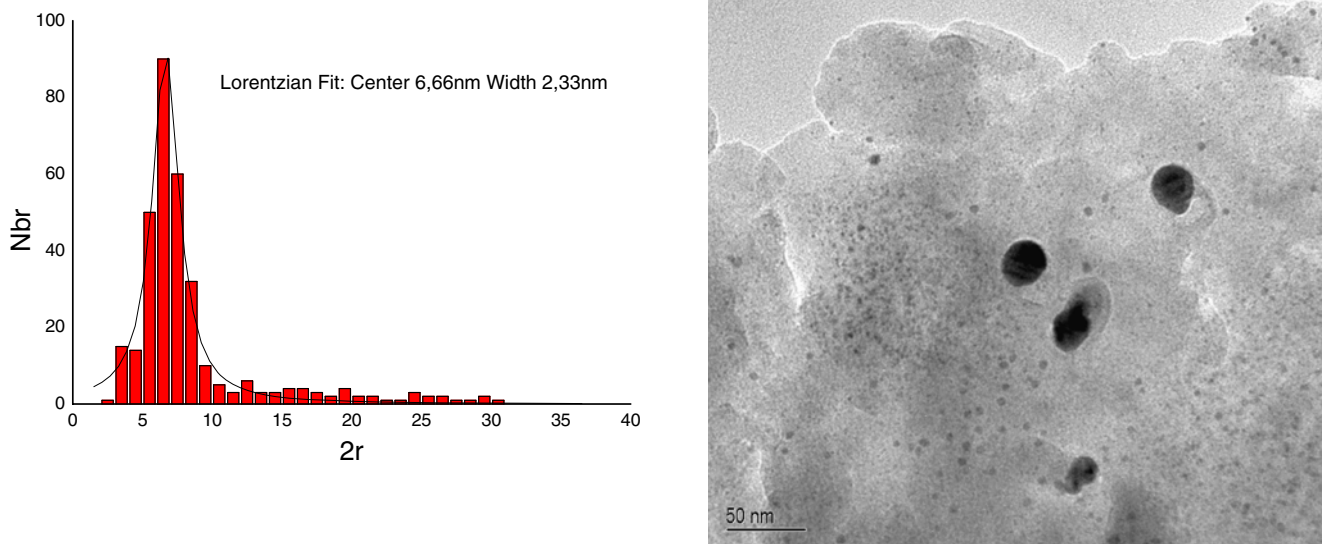


**Fig. 4** Size distribution and TEM image of the sample annealed for 2 h. A Lorentzian law is used to fit the distribution

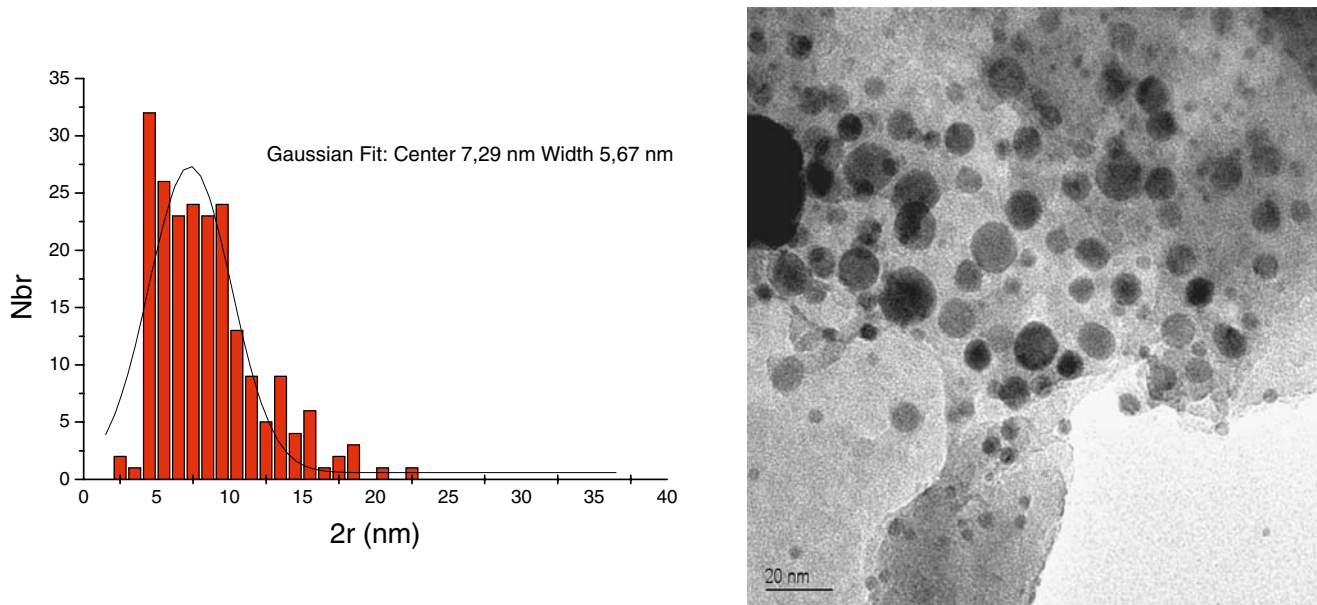


**Fig. 5** Size distribution and TEM image of the sample annealed for 3 h. A Gaussian law is used to fit the distribution

From TEM observations, size histogram and imaging versus annealing have been plotted in Figs. 3, 4, 5, and 6 using Digital Micrograph Software. We can observe an increase in the mean particle size from 4.71 nm at 1 h to 12 nm at 4 h for the biggest particles. For this duration, a second population is observed centered around 5 nm. A broadening of the bandwidth with time is also visible particularly at 4 h. However, the particle distribution better fit is obtained here with a mixing of Gaussian and

Lorentzian function and leads to two particles population. The particle shape is initially spherical for 1 to 3-h cases and is changing for the biggest one with facets apparition in Fig. 7.

The size evolution versus the annealing time is plotted in Fig. 7. For times between 1 and 3 h, the evolution is ascribed to a diffusion law with an evolution in  $d^2$  [14–16], and after 3 h, this evolution is faster and ascribed to an Oswald growth in volume for the biggest particles [17–19].

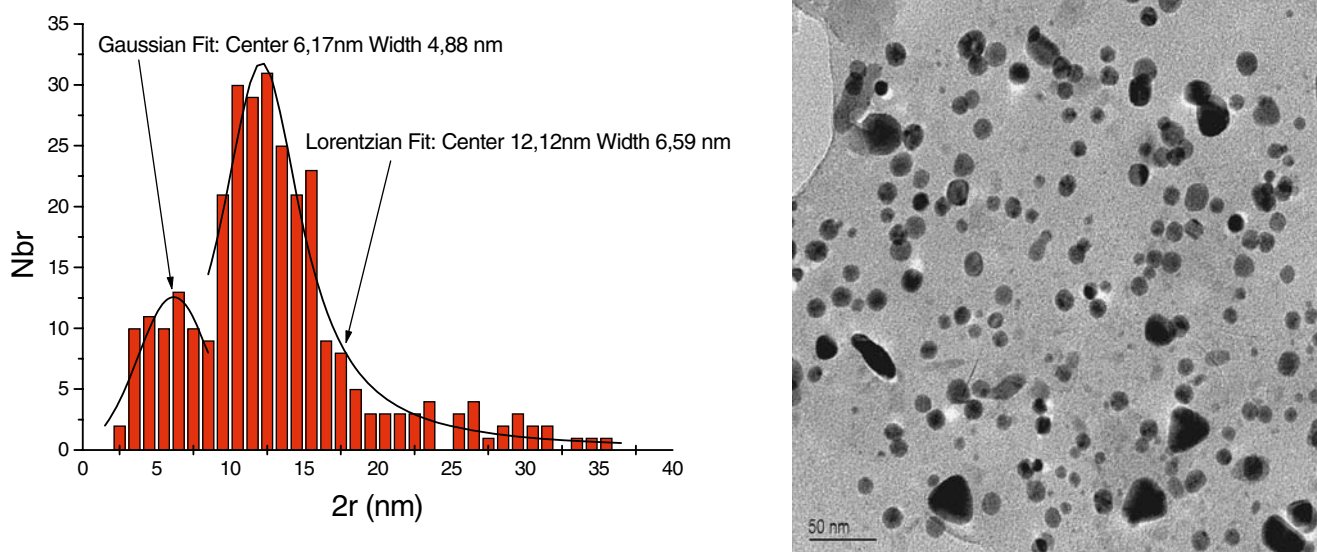


**Fig. 6** Size distribution and TEM image of the sample annealed for 4 h. Gaussian and Lorentzian laws are used to fit the distribution

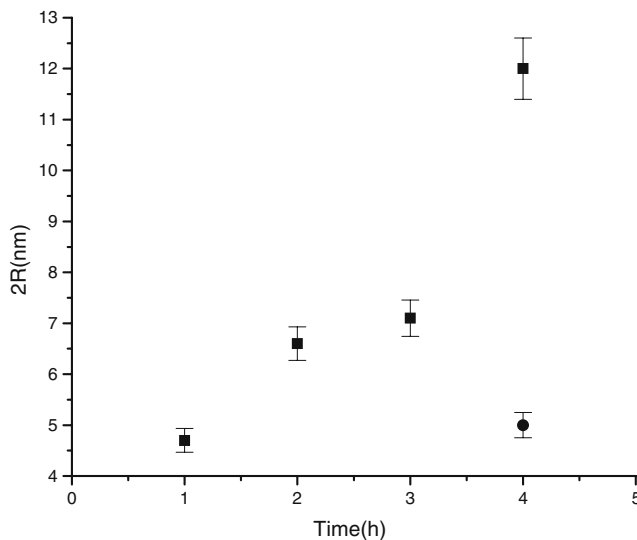


**Fig. 7** Particles size evolution with the annealing time (annealing temperature of 500 °C)

## Discussion

The absorption peaks are due to the surface plasmon resonance of silver cluster. The size distribution particles is dominated by a mean size  $R$ , increasing with time, with volume fraction  $N$ , which gives the absorption intensity, as a function of the absorption cross-section  $\sigma$ :

$$A = N \cdot \sigma \cdot l \quad (1)$$

where  $N$  is the particle density in the matrix, and  $l$  is the thickness of the sample.

According to Drude model [20], absorption cross-section  $\sigma(\lambda, R)$  of silver nanoclusters at wavelength  $\lambda$  varies with mean size particle  $R$  as:

$$\sigma(\lambda, R) = \frac{18 \pi V n^3}{\lambda} \frac{\varepsilon_2}{(\varepsilon_1 + 2n^2)^2 + \varepsilon_2^2} [\text{cm}^{-1}] \quad (2)$$

where the metal dielectric function is given by

$$\begin{aligned} \varepsilon_{\text{Drude}}(\omega) &= 1 - \frac{\omega_p^2}{\omega^2 + i\Gamma_{\text{Bulk}}(R)\omega} \\ &\equiv \varepsilon_{1,\text{Drude}}(\omega) + i\varepsilon_{2,\text{Drude}}(\omega) \end{aligned} \quad (3)$$

with

$$\begin{cases} \varepsilon_{1,\text{Drude}}(\omega) = 1 - \frac{\omega_p^2}{\omega^2 + \Gamma_{\text{Bulk}}^2} \\ \varepsilon_{2,\text{Drude}}(\omega) = \frac{\omega_p^2 \Gamma_{\text{Bulk}}}{\omega^2 + \Gamma_{\text{Bulk}}^2} \end{cases} \quad (4)$$

and

$$\omega = \frac{2\pi c}{\lambda} \quad (5)$$

$V$  is the particle volume, linked to its size  $R$ ;  $\omega$ , the angular frequency;  $\omega_p$ , the plasmon resonance frequency;  $n$  is the effective dielectric constant of the matrix; and  $\Gamma_{\text{Bulk}}$  is the effective damping parameter for the free electrons in the bulk metal.

Taking into account the inter-band transitions of the metal in the expression of  $\varepsilon$  and the effect of reduction of electron mean free path when confined in particles whose size is smaller than the bulk mean free path ( $\approx 52$  nm for pure silver at 273 K [21]), we have

$$\begin{cases} \varepsilon_1(\omega, R) = \varepsilon_{1\text{Inter}} + \varepsilon_{1\text{Drude}} = \varepsilon_{1\text{Inter}} + 1 - \frac{\omega_p^2}{\omega^2 + \Gamma(\omega, R)^2} \\ \varepsilon_2(\omega, R) = \varepsilon_{2\text{Inter}} + \varepsilon_{2\text{Drude}} = \varepsilon_{2\text{Inter}} + \frac{\omega_p^2 \Gamma}{\omega^2 + \Gamma(\omega, R)^2} \end{cases} \quad (6)$$

with

$$\Gamma(R) = \Gamma_{\text{Bulk}} + A \frac{V_f}{R} \quad (7)$$

$\varepsilon_1$  and  $\varepsilon_2$  are the real and imaginary parts of the dielectric function of the nanoparticles;  $\varepsilon_{1\text{Inter}}$  and  $\varepsilon_{2\text{Inter}}$  are the real and imaginary part of the frequency dependent dielectric function of bulk silver due to the inter-band transitions;

$A$  is a model-dependent parameter ( $A=2.00$  [22]÷0.25 [23]);

$\Gamma_{\text{Bulk}}$  is the absorption coefficient of the plasmon electron, and the second term in the expression of  $\Gamma$  is used to introduce a size-dependent term in the damping frequency with the nanoparticle size  $R$ ;

$V_f$  is the Fermi velocity of electrons in bulk silver ( $V_f=1.39 \times 10^8$  cm s $^{-1}$  in the case of silver) [20].

The absorption cross-section has been compiled in Fig. 8 with  $A=1$ ,  $n=1.6$  and size between 2 and 11 nm. Clearly, the intensity increases with the particle size and confirms the TEM particle size determination and the experimental absorption curves for time between 1 and 3 h. The broadening of the bandwidth is due to the particle distribution observed in TEM from 1 to 3 h, which is not taken into account in the Drude model.

Nucleation of silver atoms can take place due to the fluctuations in the local concentrations of diffusing silver [14–16]. According to these authors, the growth of the particles between 1 and 3 h follows the typical evolution related to diffusion-controlled process [14]

$$d^2(t) = d_0^2 + 8 \frac{C_s - C_e}{C_p - C_e} D t \quad (8)$$

where  $d_0$  is the value of  $d$  at  $t=0$ ,  $C_p$  is the concentration of limiting reactant in the cluster and  $D$  is the diffusion coefficient,  $C_s$  and  $C_e$  are, respectively, the concentration for the limiting reactant before growth and the equilibrium

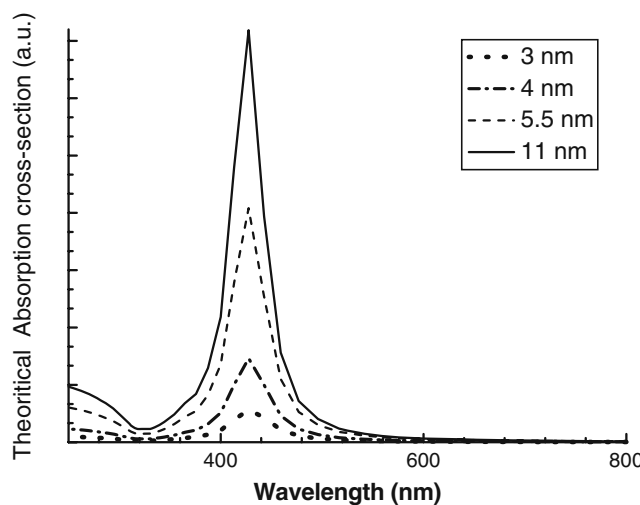


**Fig. 8** Theoretical Drude optical absorption spectra of silver nanoparticles embedded in glass for various sizes

in the matrix.  $C_p$  is the concentration for the limiting reactant in the cluster and  $D$  its diffusion coefficient. After 3 h, we reach the limit concentration in the glass, and the growth process is then governed by an Oswald law according to a process in volume [17–19]. At this stage, the particles grow in volume, and each particle stays as a single crystalline. The electron diffraction of one particle, obtained for the sample annealed during 4 h (Fig. 9), indicates that the particle is in the cubic face centered phase. The corresponding high-resolution image (Fig. 9a)

shows the 0.23-nm spacing fringes which are the (111) lattice fringes of Ag (Fig. 9b).

These results give us an explanation for the optical absorption evolution of the samples. The blue shift phenomena observed between 1 and 3 h is correlated to a diffusion process. The red shift phenomena, leading to a absorbance decrease observed at 4 h, is correlated to an Oswald process associated with change in particle distribution size and the apparition of two families and in biggest particles shape change which can lead to a depolarization factor. The size distribution observed in TEM is broadened when the annealing time increases and is directly correlated to the FWHM of the absorption curves. Moreover, the nanoparticle size is below the mean free path of the electrons in bulk silver, which proves that we are well in a confinement regime.

## Conclusion

Optical absorption in the UV–Visible range of time annealed samples were performed to see the variation of the optical properties of silver nanoparticles embedded in glass. TEM measurements were carried out to corroborate the optical evolution with the size distribution evolution. We have associated the growth law of the silver particles to the optical absorption curves and conclude in a first step to a diffusion process and in a second step to an Oswald one. The annealing time leads to the formation of two particles population and an evolution of the biggest particles shape which stays monocrystalline. These changes lead to a broadening of the absorption curve, a decrease of the intensity, and a red shift of the plasmon resonance.

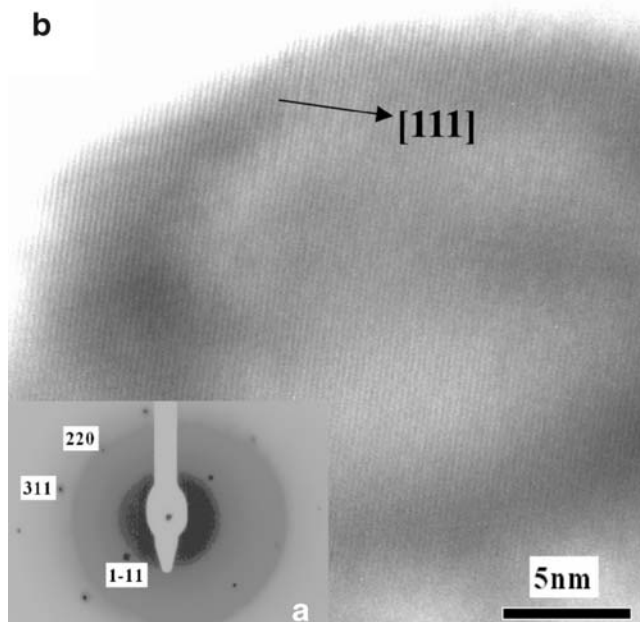


**Fig. 9** **a** Electron diffraction pattern of a particle of the sample annealed during 4 h and **b** the corresponding high-resolution image. The particle is in the [1–1–2] zone axis

## References

1. Bond GC (1985) Surf Sci 156(2):966–981
2. Mitrikas G, Deligiannakis Y, Trapalis CC, Boukos N, Kordas G (1998) J Sol–Gel Sci Technol 13:503
3. Faccio P, Trapani DI, Borsella E, Gonella F, Mazzoldi P, Malvezzi AM (1998) Europhys Lett 43:213
4. Kokkoris M, Trapalis CC, Kossionides S, Vlastou R, Nsouli B, Grotzschel R, Kordas G, Paradellis TH (2002) Nucl Instrum Methods Phys Res B 188:7
5. Kawashita M, Tsuneyama S, Miyaja F, Kokudo T, Yamamoto K (2000) Biomaterials 21:393
6. Gangopadhyay P, Kesavamoorthy R, Nair KGM, dhandapani R (2000) J Appl Phys 88:4975
7. Epifani M, Giannini C, Vasanelli L (2000) J Am Ceram Soc 83:2385
8. Miotello A, De Marchi G, Mattei G, Mazzoldi P, Quaranta A (2000) Appl Phys A 70:415
9. Gangopadhyay P, Magudapathy P, Kesavamoorthy R, Panigrahi BK, Nair KGM, Satyam PV (2004) Chem Phys Lett 388:416

10. Huidan Z, Chongjun Z, Jianrong Q, Yunxia Y, Guorong C (2007) *J Cryst Growth* 300:519–522
11. Zeng H-D, Qiu J-R, Jiang X-W, Qu S-L, Zhu C-S, Gan F-X (2003) *Chin Phys Lett* 20(6):932
12. De Marchi G, Caccavale F, Gonella F, Mattei G, Mazzoldi P, Battaglin G, Quaranta A (1996) *Appl Phys A* 63:403
13. Bottani CE, Li Bassi A, Stella A, Cheyssac P, Kofman R (2001) *Europhys Lett* 56:386
14. Gangopadhyay P, Magudapathy P, Kesavamoorthy R, Panigra BK, Nair KGM, Satyam PV (2004) *Chem Phys Lett* 388:416
15. Yukselici H, Persans PD, Hayes TM (1995) *Phys Rev B* 52:11763
16. Lifshitz IM, Slyosov VV (1961) *J Phys Chem Solids* 19(35):35
17. Wagner C (1961) *Z Elektrochem* 65:581
18. Philibert J (1985) Diffusion et transport de matière dans les solides. Les éditions de Physique
19. Snyder VA, Alkemper J, Voorhees PW (2000) *Acta Mater* 48:2689
20. Bohren CF, Huffman DR (1983) Absorption and scattering of light by small particles. Wiley Science Paperback Series, New York
21. Palpant B (1998) Thesis. University Claude Bernard, Lyon 1 (France)
22. Pinçon N, Palpant B, Prot D, Charron E, Debrus S (2002) *Eur Phys J D* 19:395
23. Pinchuk A, Kreibig U, Hilger A (2004) *Surf Sci* 557:269–280